PHYSICAL REVIEW A **94**, 030304(R) (2016)

Entangled vector vortex beams

Vincenzo D'Ambrosio,[1,2] Gonzalo Carvacho,[1] Francesco Graffitti,[1] Chiara Vitelli,[1] Bruno Piccirillo,[3,4] Lorenzo Marrucci,[3,4] and Fabio Sciarrino[1,*]

[1]*Dipartimento di Fisica, Sapienza Università di Roma, I-00185 Roma, Italy*

[2]*ICFO-Institut de Ciencies Fotoniques, The Barcelona Institute of Science and Technology, E-08860 Castelldefels, Barcelona, Spain*

[3]*Dipartimento di Fisica, Università di Napoli Federico II, Complesso Universitario di Monte S. Angelo, I-80126 Napoli, Italy*

[4]*CNR-SPIN, Complesso Universitario di Monte S. Angelo, I-80126 Napoli, Italy*

(Received 10 December 2015; published 30 September 2016)

Light beams having a vectorial field structure, or polarization, that varies over the transverse profile and a central optical singularity are called vector vortex (VV) beams and may exhibit specific properties such as focusing into "light needles" or rotation invariance. VV beams have already found applications in areas ranging from microscopy to metrology, optical trapping, nano-optics, and quantum communication. Individual photons in such beams exhibit a form of single-particle quantum entanglement between different degrees of freedom. On the other hand, the quantum states of two photons can be also entangled with each other. Here, we combine these two concepts and demonstrate the generation of quantum entanglement between two photons that are both in VV states: a form of entanglement between two complex vectorial fields. This result may lead to quantum-enhanced applications of VV beams as well as to quantum information protocols fully exploiting the vectorial features of light.

DOI: 10.1103/PhysRevA.94.030304

I. INTRODUCTION

Quantum entanglement lies at the basis of fundamental questions on the nature of reality, as exemplified by the Einstein-Podolsky-Rosen argument or the Schrödinger's cat paradox [1]. On the other hand, entangled systems are today a key tool of quantum information technology [2,3]. Entangled photon pairs, in particular, are commonly generated by exploiting nonlinear optical processes [4] and may show entanglement in several degrees of freedom, such as frequency, path, orbital angular momentum (OAM), and polarization [5]. The optical polarization, defining the oscillation directions of the electromagnetic fields, is typically approximately uniform in a light beam. Yet, the polarization can also vary over the transverse profile, giving rise to vector beams with peculiar polarization patterns [6]. The so-called vector vortex (VV) beams are a particular class of vector beams characterized by a central optical singularity surrounded by an azimuthally varying pattern of polarization [7,8]. These beams can be conveniently described as balanced, nonseparable superpositions of polarization-OAM eigenmodes, with the OAM magnitude defining the "order" of the beams. Hence, photons in VV beams are actually entangled in these two degrees of freedom: Such a kind of single-particle entanglement is also known as "intrasystem" entanglement [9–11]. The inseparability between the polarization and spatial degree of freedom of single particles is not related to nonlocal properties, therefore, it is not possible to perform a nonlocality test on these states [12]. Nevertheless, violations of Bell-like inequalities can be exploited for a single system in order to certify the presence of single-particle entanglement [13], particularly for photonic systems [11,14].

VV beams have already found applications in areas ranging from microscopy [15] to metrology [16,17], optical trapping [18], nano-optics [19], and quantum communication [20–22]. Due to their interesting properties, in the last years several techniques have been developed to generate, manipulate, and analyze VV beams [7,8,23–26]. In this Rapid Communication, we report the generation and characterization of entangled pairs of VV photons of arbitrary order. In particular, we consider five combinations of VV mode orders, corresponding to different polarization patterns for the two beams. We simultaneously demonstrate, by complete 16-dimensional quantum tomography, both the *intrasystem* entanglement between the polarization and OAM within each photon and the *intersystem* entanglement between the two photon states: The former is related to the structure of VV states, and the latter corresponds to entanglement between two complex vectorial fields. Finally, by performing a nonlocality test directly in the VV space, we show that entanglement between complex vectorial fields can be effectively exploited as a resource in fundamental quantum mechanics as well as quantum information.

II. VECTOR VORTEX BEAM GENERATION

Let us denote with $|R,\ell\rangle$ ($|L,\ell\rangle$) the state of a photon with uniform right (left) circular polarization carrying $\ell\hbar$ of orbital angular momentum. A VV beam of order m is defined in the two-dimensional Hilbert space spanned by $\{|R,m\rangle, |L,-m\rangle\}$. In particular, we consider the two balanced superpositions $|\hat{r}_m\rangle = \frac{1}{\sqrt{2}}(|R,m\rangle + |L,-m\rangle)$, $|\hat{\vartheta}_m\rangle = \frac{1}{\sqrt{2}}(|R,m\rangle - |L,-m\rangle)$. When $m=1$, the states $|\hat{r}_1\rangle$ and $|\hat{\vartheta}_1\rangle$ correspond to the well-known radially and azimuthally polarized beams [7]. For brevity, we will refer to states $|\hat{r}_m\rangle$ and $|\hat{\vartheta}_m\rangle$ with the terms "radial" and "azimuthal," irrespective of m. A generic VV beam (or photon VV state) can be represented on a "hybrid Poincaré sphere" (HPS) [27,28], where states $\{|R,m\rangle, |L,-m\rangle\}$ lie on the poles and $|\hat{r}_m\rangle$ and $|\hat{\vartheta}_m\rangle$ lie on opposite points on the equator. Figure 1 shows examples of

*fabio.sciarrino@uniroma1.it

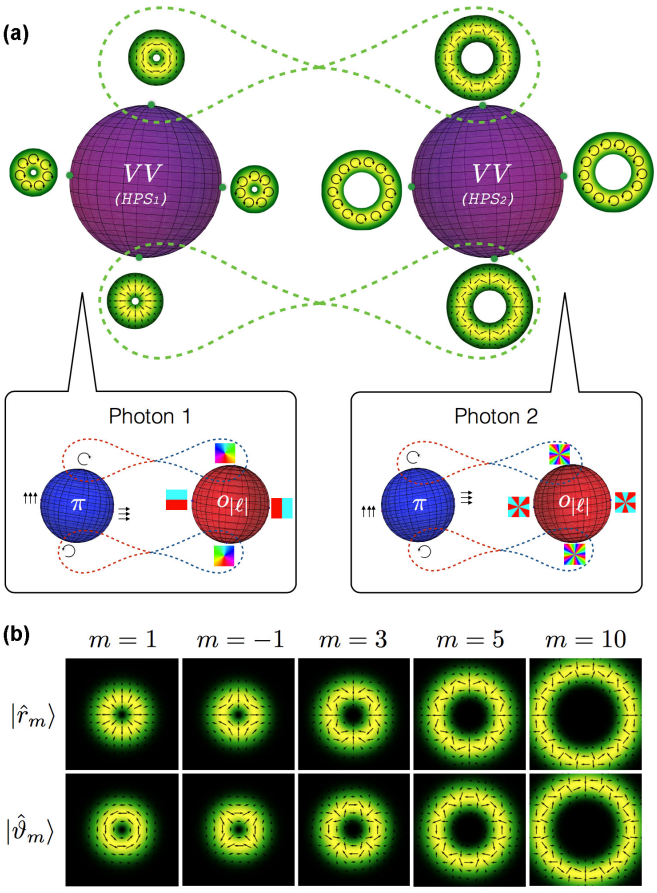

FIG. 1. Representation of entangled VV beams and their underlying intrasystem entanglement structure. (a) shows the intersystem entanglement (green dashed lines) between VV beams belonging to different orders. Each VV state is defined on a hybrid Poincaré sphere: purple spheres HPS_1 and HPS_2, corresponding to orders $m = 1$ and $m = 5$, respectively, represented together with the intensity and polarization patterns for the corresponding azimuthal, radial, and circularly polarized modes (for graphical reasons, these spheres are oriented with the two poles corresponding to polarization-OAM eigenstates aligned in the horizontal direction). The Poincaré spheres in the two lower boxes represent the polarization π (blue spheres) and OAM $o_{|\ell|}$ (red spheres) spaces within each photon, with their respective polarization patterns and phase profiles. The intrasystem entanglement (blue/red dashed lines) between these two degrees of freedom of the single photons generates the VV states. (b) reports the intensity and polarization patterns of radial and azimuthal VV beams of various orders.

this representation and the polarization and intensity patterns of some of these modes. By noticing that the complete polarization-OAM Hilbert space of order m is spanned by the four states $\{|R,m\rangle, |L,-m\rangle, |L,m\rangle, |R,-m\rangle\}$, we can also define π modes [18] of order m as balanced superpositions in the space spanned by $\{|R,-m\rangle, |L,m\rangle\}$: $|\hat{\pi}_m^+\rangle = \frac{1}{\sqrt{2}}(|R,-m\rangle + |L,m\rangle)$ and $|\hat{\pi}_m^-\rangle = \frac{1}{\sqrt{2}}(|R,-m\rangle - |L,m\rangle)$.

In this Rapid Communication, we generate and detect VV modes by using a specialized optical component, the q plate, a birefringent patterned slab that can couple or decouple the polarization and OAM of single photons [29]. In more detail, a q plate with a topological charge q maps a photon with the input state $\alpha|R,0\rangle + \beta|L,0\rangle$ into the output state $\alpha|L,-2q\rangle + \beta|R,2q\rangle$ and vice versa. Thus, radial and azimuthal VV beams $|\hat{r}_m\rangle$ and $|\hat{\vartheta}_m\rangle$ are easily produced by using a linear horizontal (H) and vertical (V) input polarization, respectively, with $m = 2q$. A q plate can also be used to measure VV beams. Indeed, a radial (azimuthal) VV beam of order m is transformed into a linear horizontal (vertical) uniformly polarized beam by a q plate with $2q = m$. In this way, the measurement of a complex polarization pattern such as that of a VV beam is reduced to a much simpler polarization measurement [8,26]. A more general and complete approach to analyze VV beams is by measuring separately the polarization and OAM, for instance, by performing a quantum state tomography in the complete polarization-OAM Hilbert space. More complex polarization structures where polarization is linked to a larger OAM subspace could be eventually investigated by exploiting more complex experimental setups (involving, for instance, spatial light modulators or several q plates in a cascade configuration).

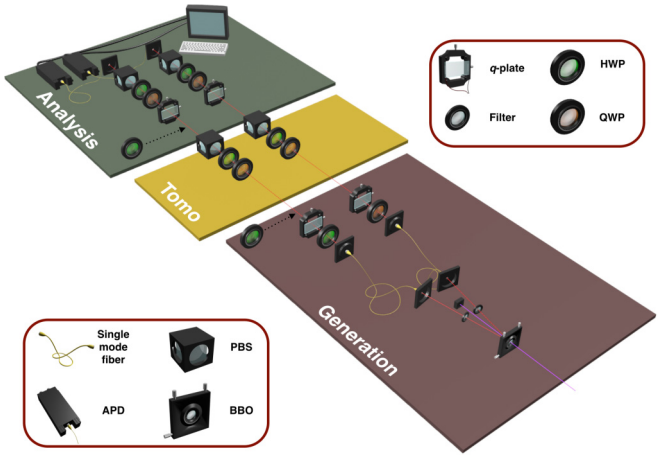

FIG. 2. Experimental apparatus for the generation and analysis of entangled VV photons. In the generation stage, a polarization-entangled photon pair is produced in a BBO crystal and is then converted into a VV-entangled pair by two q plates. The generation of a π mode needs an additional HWP after the q plate. The Tomo section corresponds to a polarization-analysis stage formed by a quarter-wave plate (QWP), a HWP, and a polarizer (PBS). This section is used only for the full tomography in the complete polarization-OAM space, while it is not needed for direct VV-space measurements. The analysis stage deals with the OAM- or VV-mode analysis (it is OAM mode if the Tomo stage is inserted, otherwise it is VV mode): On each arm a q plate converts back the OAM or VV modes into uniform polarization states, which are then measured with a polarization-analysis stage. The photons are then coupled into a single-mode fiber that filters the non-Gaussian modes and are sent to single-photon detectors.

Our experimental apparatus is depicted in Fig. 2. In the generation section a polarization-entangled photon pair is produced by exploiting spontaneous parametric down conversion in a β-barium-borate crystal (BBO) [4]. After the crystal, both photons are filtered in the wavelength, via a narrowband interference filter, and in the spatial mode, via a single-mode fiber. This last operation sets the transverse mode of both

photons to a fundamental Gaussian one, corresponding to vanishing OAM. As a last step, two q plates with topological charges q_1 and q_2 transform the two polarization photon states into VV modes of orders $m_1 = 2q_1$ and $m_2 = 2q_2$, respectively. The resulting state emerging from the source is

$$|\Psi^{-}_{m_1,m_2}\rangle = \frac{1}{\sqrt{2}}(|\hat{r}_{m_1}\rangle_1 |\hat{\vartheta}_{m_2}\rangle_2 - |\hat{\vartheta}_{m_1}\rangle_1 |\hat{r}_{m_2}\rangle_2), \qquad (1)$$

which corresponds to a pair of entangled vector vortex beams of orders m_1 and m_2. A set of maximally entangled VV states can be easily obtained by performing local operations on the photons (see the Supplemental Material [30]).

To prove the generality of our approach, we generated various combinations of VV mode orders (m_1,m_2): (1,1), (1,5), (1,10), and (3,5). Finally, we considered the pair $(1, -1)$. The VV modes with $m < 0$ (π modes) can be obtained by flipping the circular polarization handedness with a half-wave plate (HWP) added after the q plate.

III. QUANTIFICATION OF INTRASYSTEM AND INTERSYSTEM ENTANGLEMENT

To fully analyze the entangled pairs, we performed quantum state tomography in the polarization and the OAM subspaces corresponding to the VV mode of each photon. In this way it is possible to measure both the intrasystem and the intersystem entanglement of our states, certifying the generation of entanglement between complex vectorial fields. The corresponding experimental setup is shown in Fig. 2 (Tomo and analysis sections). After a polarization-analysis stage (two wave plates and a polarizer), each photon is sent to a q plate and a second polarization-analysis stage. In this configuration, the q plate transfers the information initially written in the OAM subspace into the polarization state of the photon that can be then analyzed with standard techniques [31,32]. An overcomplete set of measurements of polarization and OAM for both photons (1296 settings overall) has been performed to fully reconstruct the density matrix of the entangled photon pair in the 16-dimensional Hilbert space (see the Supplemental Material [30]). The comparison between experimental and theoretical density matrices is reported in Fig. 3(a) for two VV combinations. The complete set of experimental density matrices can be found in the Supplemental Material [30]. The quality of our states can be expressed through the fidelity $F = \mathrm{Tr}[\sqrt{\sqrt{\rho_{\mathrm{theo}}}\rho_{\mathrm{expt}}\sqrt{\rho_{\mathrm{theo}}}}]$ between the experimental density matrix (ρ_{expt}) and the corresponding theoretical one (ρ_{theo}). The average fidelity is $F = 0.97 \pm 0.01$.

In order to quantify the intrasystem entanglement of VV states, we estimated the concurrence C for the single-photon reduced density matrix in the polarization-OAM space after a projective measurement performed on the other photon onto the states of the mutually unbiased bases used for the tomography. Figure 3(b) shows the concurrence distribution for each photon when the other is projected over 34 different states $\{\chi_i\}$. As expected, the distribution is divided in two regions (blue and orange) corresponding to entangled ($C = 1$) and separable ($C = 0$) states, respectively (the difference from theoretical values is due to experimental imperfections). Indeed, when χ_i contains a circular polarized state or a OAM

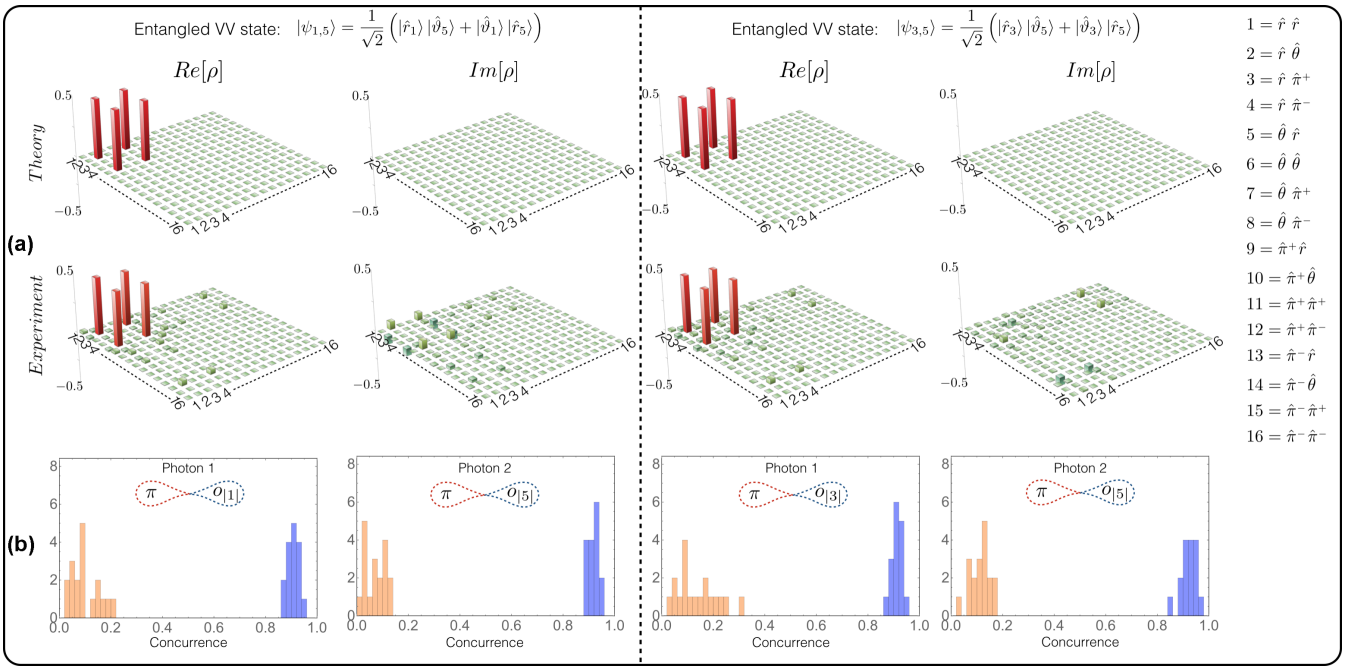

FIG. 3. Experimental results. (a) Experimental and theoretical density matrices for entangled VV beams of orders ($m_1 = 1$,$m_2 = 5$) (on the left) and ($m_1 = 3$,$m_2 = 5$) (on the right). The first (second) element of the entries in the density matrices corresponds to the first (second) photon in the vector vortex state which can be in a radial, azimuthal, or π mode. (b) Polarization-OAM concurrence distributions. To quantify the intrasystem entanglement we calculated the concurrence distributions for the single-photon reduced density matrix after 34 different projective measurements performed on the other photon. All the distributions are divided in two regions corresponding to entangled (blue) and separable (orange) states.

TABLE I. Intersystem concurrences for entangled VV beams of different orders.

(m_1,m_2)	Concurrence
(1,1)	0.949 ± 0.003
(1,5)	0.906 ± 0.003
(1,10)	0.863 ± 0.003
(3,5)	0.908 ± 0.002
$(1,-1)$	0.914 ± 0.003

eigenstate, the state of the other photon is separable, while in the other case (i.e., the linear and diagonal polarization and their counterpart in the OAM space), it is a maximally entangled state corresponding to a vector vortex field. If the projections are not conditioned to the states of the tomography, one may obtain any value of concurrence between 0 and 1.

On the other hand, the intersystem entanglement between two VV beams can be quantified by directly calculating the concurrence C for the corresponding density matrix in the VV space. The results for the different pairs of VV modes are shown in Table I. These values were obtained after performing a projection over the four-dimensional subspace spanned by $\{|\hat{r}_{m1}\rangle|\hat{r}_{m2}\rangle, |\hat{r}_{m1}\rangle|\hat{\vartheta}_{m2}\rangle, |\hat{\vartheta}_{m1}\rangle|\hat{r}_{m2}\rangle, |\hat{\vartheta}_{m1}\rangle|\hat{\vartheta}_{m2}\rangle\}$ of the VV beam for the cases with $m = 1,3,5,10$ and over the subspace spanned by $\{|\hat{r}_{m1}\rangle|\hat{\pi}^{+}_{m2}\rangle, |\hat{r}_{m1}\rangle|\hat{\pi}^{-}_{m2}\rangle, |\hat{\vartheta}_{m1}\rangle|\hat{\pi}^{+}_{m2}\rangle, |\hat{\vartheta}_{m1}\rangle|\hat{\pi}^{-}_{m2}\rangle\}$ for the particular case of the π mode ($m_1 = 1, m_2 = -1$).

IV. NONLOCALITY TEST

Beside the intriguing fundamental aspects of the entanglement, this feature is also a keystone in quantum-based technologies. In particular, Bell's inequalities play a fundamental role in quantum key distribution due to their capability of detecting some classes of entangled states and simultaneously testing the nonlocal nature of the system itself [33,34]. Hence we performed a nonlocality test for each pair of VV photons in order to show that entanglement between complex vectorial fields constitutes an exploitable resource in quantum protocols.

In more detail, we performed a violation of the Clauser-Horne-Shimony-Holt (CHSH) inequality [35] that sets a bound for a parameter S ($S \leqslant 2$) based on the correlations between local measurements on two photons in a separable state. The maximum violation of the CHSH inequality is given by maximally entangled states corresponding to the value $S = 2\sqrt{2}$. Experimentally, we performed projective measurements directly in the VV space by exploiting a q plate as an interface between VV and polarization spaces (analysis stage in Fig. 2). For a given VV order m, a q plate with $q = m/2$ followed by a HWP and a polarizer (PBS) allows one to implement a projective measurement on a state of the form $\cos(\gamma)|0\rangle + \sin(\gamma)|1\rangle$, for different values of γ as requested in the CHSH inequality (see the Supplemental Material [30]). The experimental values of S are reported in Table II and correspond to a violation of CHSH inequality by 39–73 standard deviations, without any correction due to dark counts.

TABLE II. Measured S parameter for CHSH inequalities using different orders of VV beams (first column) for raw data and for data corrected for dark counts (second and third columns, respectively).

(m_1,m_2)	S (raw data)	S_{corr}
(1,1)	2.654 ± 0.009	2.727 ± 0.009
(1,5)	2.649 ± 0.013	2.738 ± 0.014
(1,10)	2.437 ± 0.010	2.591 ± 0.011
(3,5)	2.621 ± 0.016	2.716 ± 0.017
$(1,-1)$	2.592 ± 0.010	2.664 ± 0.010

V. CONCLUSIONS

In this Rapid Communication we have fully investigated the entanglement properties of a photonic system composed of two entangled VV beams. Such a system shows two different types of entanglement: An intrasystem entanglement between the polarization and OAM of each photon is responsible for the complex polarization pattern of VV beams, and the two photons are also entangled with each other via an intersystem entanglement which lies at the basis of the nonlocality concept. We investigated the structure of our system by performing a full state tomography and quantifying both types of entanglement. Moreover, we performed a nonlocality test to prove that entanglement between complex vectorial fields can be used as a resource in quantum protocols.

This study paves the way towards a quantum enhancement in VV beam applications as well as the realization of different quantum information protocols that can take advantage of the combined action of both intrasystem and intersystem entanglement. Among the possibilities opened by entangled VV beams, there are, for instance, quantum teleportation [36] without a shared reference frame and enhancement in remote sensing applications. Other possible applications involve the fields of plasmonics [37] and nanoscale waveguides [38]: Indeed, it has been demonstrated that the angular momentum and polarization entanglement can be preserved in conversions such as photon-surface plasmon-photon through metal hole arrays and to hybrid nanoscale plasmonic waveguides, respectively. Moreover, with opportune engineering, the VV photons generated in our work could be a resource for high-dimensional multiphoton entanglement [39] in order to increase the dimensionality and generate layered quantum protocols due to the nonsymmetric structure of the entanglement taking advantage of the hybrid nature of these complex vectorial fields. Finally, since entangled VV photons are a bipartite system with a high-dimensional local structure, such photonic systems can constitute a reliable probe for experimental investigations on the connections between nonlocality [40] and contextuality [41–46], two important concepts in fundamental physics.

ACKNOWLEDGMENTS

We thank G. Rubino for her contribution in the preliminary stage of the experiment. This work was supported by the ERC (Belgium)-Starting Grant 3D-QUEST (3D-Quantum Integrated Optical Simulation; Grant Agreement No. 307783): PRIN 2009 (Progetti di Ricerca di Interesse Nazionale 2009), and project AQUASIM (Advanced Quantum Simulation and Metrology).

[1] R. Horodecki, P. Horodecki, M. Horodecki, and K. Horodecki, Quantum entanglement, Rev. Mod. Phys. **81**, 865 (2009).

[2] J. T. Barreiro, T. C. Wei, and P. G. Kwiat, Beating the channel capacity limit for linear photonic superdense coding, Nat. Phys. **4**, 282 (2008).

[3] T. Ladd *et al.*, Quantum computers, Nature (London) **464**, 45 (2010).

[4] P. G. Kwiat *et al.*, New High-Intensity Source of Polarization-Entangled Photon Pairs, Phys. Rev. Lett. **75**, 4337 (1995).

[5] J.-W. Pan *et al.*, Multiphoton entanglement and interferometry, Rev. Mod. Phys. **84**, 777 (2012).

[6] M. R. Dennis, K. O'Holleran, and M. J. Padgett, Singular optics: Optical vortices and polarization singularities, Prog. Opt. **53**, 293 (2009).

[7] Q. Zhan, Cylindrical vector beams: From mathematical concepts to applications, Adv. Opt. Photonics **1**, 1 (2009).

[8] F. Cardano *et al.*, Polarization pattern of vector vortex beams generated by q-plates with different topological charges, Appl. Opt. **51**, C1 (2012).

[9] A. Aiello, F. Töppel, C. Marquardt, E. Giacobino, and G. Leuchs, Quantum-like nonseparable structures in optical beams, New J. Phys. **17**, 043024 (2015).

[10] M. McLaren, T. Konrad, and A. Forbes, Measuring the nonseparability of vector vortex beams, Phys. Rev. A **92**, 023833 (2015).

[11] E. Karimi, J. Leach, S. Slussarenko, B. Piccirillo, L. Marrucci, L. Chen, W. She, S. Franke-Arnold, M. J. Padgett, and E. Santamato, Spin-orbit hybrid entanglement of photons and quantum contextuality, Phys. Rev. A **82**, 022115 (2010).

[12] R. J. C. Spreeuw, Classical wave-optics analogy of quantum-information processing, Phys. Rev. A **63**, 062302 (2001).

[13] Y. Hasegawa *et al.*, Violation of a Bell-like inequality in single-neutron interferometry, Nature (London) **425**, 45 (2003).

[14] C. V. S. Borges, M. Hor-Meyll, J. A. O. Huguenin, and A. Z. Khoury, Bell-like inequality for the spin-orbit separability of a laser beam, Phys. Rev. A **82**, 033833 (2010).

[15] A. F. Abouraddy and K. C. Toussaint, Jr., Three-Dimensional Polarization Control in Microscopy, Phys. Rev. Lett. **96**, 153901 (2006).

[16] V. D'Ambrosio *et al.*, Photonic polarization gears for ultra-sensitive angular measurements, Nat. Commun. **4**, 2432 (2013).

[17] F. K. Fatemi, Cylindrical vector beams for rapid polarization-dependent measurements in atomic systems, Opt. Express **19**, 25143 (2011).

[18] B. J. Roxworthy and K. C. Toussaint, Jr., Optical trapping with π-phase cylindrical vector beams, New J. Phys. **12**, 073012 (2010).

[19] M. Neugebauer, T. Bauer, P. Banzer, and G. Leuchs, Polarization tailored light driven directional optical nanobeacon, Nano Lett. **14**, 2546 (2014).

[20] V. D'Ambrosio *et al.*, Complete experimental toolbox for alignment-free quantum communication, Nat. Commun. **3**, 961 (2012).

[21] G. Vallone, V. D'Ambrosio, A. Sponselli, S. Slussarenko, L. Marrucci, F. Sciarrino, and P. Villoresi, Free-Space Quantum Key Distribution by Rotation-Invariant Twisted Photons, Phys. Rev. Lett. **113**, 060503 (2014).

[22] V. Parigi *et al.*, Storage and retrieval of vector beams of light in a multiple-degree-of-freedom quantum memory, Nat. Commun. **6**, 7706 (2015).

[23] C. Maurer, A. Jesacher, S. Fürhapter, S. Bernet, and M. Ritsch-Marte, Tailoring of arbitrary optical vector beams, New J. Phys. **9**, 78 (2007).

[24] R. Fickler, R. Lapkiewicz, S. Ramelow, and A. Zeilinger, Quantum entanglement of complex photon polarization patterns in vector beams, Phys. Rev. A **89**, 060301 (2014).

[25] J. T. Barreiro, T.-C. Wei, and P. G. Kwiat, Remote Preparation of Single-Photon "Hybrid" Entangled and Vector-Polarization States, Phys. Rev. Lett. **105**, 030407 (2010).

[26] V. D'Ambrosio, F. Baccari, S. Slussarenko, L. Marrucci, and F. Sciarrino, Arbitrary, direct and deterministic manipulation of vector beams via electrically-tuned q-plates, Sci. Rep. **5**, 7840 (2015).

[27] A. Holleczek, A. Aiello, C. Gabriel, C. Marquardt, and G. Leuchs, Classical and quantum properties of cylindrically polarized states of light, Opt. Express **19**, 9714 (2011).

[28] G. Milione, H. I. Sztul, D. A. Nolan, and R. R. Alfano, Higher-Order Poincaré Sphere, Stokes Parameters, and the Angular Momentum of Light, Phys. Rev. Lett. **107**, 053601 (2011).

[29] L. Marrucci, C. Manzo, and D. Paparo, Optical Spin-to-Orbital Angular Momentum Conversion in Inhomogeneous Anisotropic Media, Phys. Rev. Lett. **96**, 163905 (2006).

[30] See Supplemental Material at http://link.aps.org/supplemental/10.1103/PhysRevA.94.030304 for technical details and the complete set of experimental density matrices.

[31] E. Nagali, F. Sciarrino, F. DeMartini, L. Marrucci, B. Piccirillo, E. Karimi, and E. Santamato, Quantum Information Transfer from Spin to Orbital Angular Momentum of Photons, Phys. Rev. Lett. **103**, 013601 (2009).

[32] V. D'Ambrosio *et al.*, Deterministic qubit transfer between orbital and spin angular momentum of single photons, Opt. Lett. **37**, 172 (2012).

[33] N. Gisin, G. Ribordy, W. Tittel, and H. Zbinden, Quantum Cryptography, Rev. Mod. Phys. **74**, 145 (2002).

[34] C. Brukner, M. Żukowski, J. W. Pan, and A. Zeilinger, Bell's Inequalities and Quantum Communication Complexity, Phys. Rev. Lett. **92**, 127901 (2004).

[35] J. F. Clauser, M. A. Horne, A. Shimony, and R. A. Holt, Proposed Experiment to Test Local Hidden-Variable Theories, Phys. Rev. Lett. **23**, 880 (1969).

[36] S. Pirandola, J. Eisert, C. Weedbrook, A. Furusawa, and S. L. Braunstein, Advances in quantum teleportation, Nat. Photonics **9**, 641 (2015).

[37] X. F. Ren, G. P. Guo, Y. F. Huang, C. F. Li, and G. C. Guo, Plasmon-assisted transmission of high-dimensional orbital angular-momentum entangled state, Europhys. Lett. **76**, 753 (2006).

[38] M. Li, C. L. Zou, X. F. Ren, X. Xiong, Y. Y. Cai, G. P. Guo, L. M. Tong, and G. C. Guo, Transmission of photonic quantum polarization entanglement in a nanoscale hybrid plasmonic waveguide, Nano Lett. **15**, 2380 (2015).

[39] M. Malik, M. Erhard, M. Huber, M. Krenn, R. Fickler, and A. Zeilinger, Multi-photon entanglement in high dimensions, Nat. Photonics **10**, 248 (2016).

[40] S. Popescu, Nonlocality beyond quantum mechanics, Nat. Phys. **10**, 264 (2014).

[41] M. Howard, J. Wallman, V. Victor, and J. Emerson, Contextuality supplies the 'magic' for quantum computation, Nature (London) **510**, 351 (2014).

[42] G. Kirchmair, F. Zähringer, R. Gerritsma, M. Kleinmann, O. Gühne, A. Cabello, R. Blatt, and C. F. Roos, State-independent experimental test of quantum contextuality, Nature (London) **460**, 494 (2009).

[43] R. Lapkiewicz *et al.*, Experimental non-classicality of an indivisible quantum system, Nature (London) **474**, 490 (2011).

[44] E. Amselem, M. Rådmark, M. Bourennane, and A. Cabello, State-Independent Quantum Contextuality with Single Photons, Phys. Rev. Lett. **103**, 160405 (2009).

[45] E. Nagali, V. D'Ambrosio, F. Sciarrino, and A. Cabello, Experimental Observation of Impossible-To-Beat Quantum Advantage on a Hybrid Photonic System, Phys. Rev. Lett. **108**, 090501 (2012).

[46] V. D'Ambrosio, I. Herbauts, E. Amselem, E. Nagali, M. Bourennane, F. Sciarrino, and A. Cabello, Experimental Implementation of a Kochen-Specker Set of Quantum Tests, Phys. Rev. X **3**, 011012 (2013).